



Progress and remaining challenges in high-throughput volume electron microscopy

Jörgen Kornfeld and Winfried Denk

Recent advances in the effectiveness of the automatic extraction of neural circuits from volume electron microscopy data have made us more optimistic that the goal of reconstructing the nervous system of an entire adult mammal (or bird) brain can be achieved in the next decade. The progress on the data analysis side — based mostly on variants of convolutional neural networks — has been particularly impressive, but improvements in the quality and spatial extent of published VEM datasets are substantial. Methodologically, the combination of hot-knife sample partitioning and ion milling stands out as a conceptual advance while the multi-beam scanning electron microscope promises to remove the data-acquisition bottleneck.

Address

Max Planck Institute of Neurobiology, Am Klopferspitz 18,
 82152 Planegg, Germany

Corresponding author: Kornfeld, Jörgen (kornfeld@neuro.mpg.de)

Current Opinion in Neurobiology 2018, **50**:261–267

This review comes from a themed issue on **Neurotechnologies**

Edited by **Polina Anikeeva** and **Liqun Luo**

For a complete overview see the [Issue](#) and the [Editorial](#)

Available online 12th May 2018

<https://doi.org/10.1016/j.conb.2018.04.030>

0959-4388/© 2018 The Authors. Published by Elsevier Ltd. This is an open access article under the CC BY license (<http://creativecommons.org/licenses/by/4.0/>).

Introduction

Only 30 years after their development began in earnest [1], self-driving cars, controlled by sophisticated artificial intelligence (AI) algorithms, now cause serious accidents at a rate that roughly matches that seen for human drivers, at least according to a manufacturer's press release (Tesla; URL: <https://www.tesla.com/blog/tragic-loss>). Natural intelligence (NI) depends on the brain, with algorithms (and probably memory as well [2]), that are encoded to some, possibly overwhelming, degree in the connection pattern between neurons. Those connections are made by synapses but depend on neural wires (axons and dendrites) for their link to the cell soma. When trying to reconstruct neural wiring from volume electron microscopy (VEM) data, a computer using the best current AI algorithms [3••] makes errors at about the rate of a moderately motivated human. However, most human tracing errors are due to inattention and thus uncorrelated

[4], which means that they can be corrected by redundant tracing. Different computer algorithms, on the other hand, tend to fail at the same places in the data set, where disambiguation typically requires context and high-level knowledge that currently only human experts can provide (but see [5]). For VEM data of sufficient quality (with respect to resolution and signal-to-noise ratio (SNR)) highly motivated and knowledgeable humans, such as late-term graduate students and post-docs, can consistently (across experts) correct almost all of those errors. We can, therefore, assume that such data contain all the information needed to extract the neural circuit diagram and we can expect that algorithms will eventually be able to reconstruct at a human expert's error rate.

Progress in the analysis of VEM data

For the reconstruction of axons and dendrites, VEM-based connectomics (the only approach we will discuss here, for others see [6–8]) has in the past almost exclusively relied on a hybrid approach: first, the computer creates a candidate segmentation with parameters set to ensure that at most a few of the generated segments (supervoxels) span (merge) more than one real neurite, but each neurite is still broken up (split) into many supervoxels [9–12]. This situation is called an over segmentation and human proofreading can be performed by simply inspecting each segment for locations where it should be combined with one or more of its neighbors [13–15]. A different approach to 'proof reading' is to generate center-line tracings (skeletons), one for each neurite [4,12]. In a separate step, each skeleton is then used to combine overlapping supervoxels into a volume model of the corresponding neurite [10,12]. Both approaches yield similar results and consume about the same amount of human time (at least about 0.5 h per mm of neurite) with a possible advantage for skeletonization as long as the supervoxels are small [12,16] (for yet another approach see [17•]). This is not too surprising since both approaches require that all locations in the VEM data set are viewed by one or more humans. Note that proofreading is orders of magnitude faster than the rate at which segmentation proceeded in the case of *C. elegans* [18], where neither acquisition nor analysis used computers.

To move beyond the complete-viewing limit one has to stop proofreading decisions that the computer made on the basis of clear evidence and instead concentrate on decisions that could easily have gone the other way.

Confidence information, which may have to be generated separately [19,20], is needed to steer human inspection (Figure 1a) to ambiguous locations [13]. This has, in some cases, reduced the total proofreading effort needed to reach a given reconstruction reliability by orders of magnitude (J Kornfeld *et al.*, unpublished observations).

In addition to an increased use of targeted proofreading, there has been a recent surge in the efficacy of machine segmentation itself. It is likely that this has to do with a renewed focus on the key step in segmentation: the detection of cell boundaries (CREMI challenge; URL: <https://cremi.org/>). Boundary locations can sometimes be identified simply by testing whether the voxel intensity is above or below a certain threshold (some early connectomics data sets even made use of special staining protocols that enhanced boundary contrast [10,21]). When that fails, one can, in addition, consider the staining pattern surrounding the voxel in question, a task well suited for machine learning based on convolutional neural networks (CNNs). Finally, one can ask whether making the currently considered voxel a boundary voxel makes the local boundary shape more plausible or less so. That is what any human annotator's visual system does after having seen some amount of data from neural tissue. Expert annotators, in addition, draw on neurobiological knowledge (typical neurite diameters, neurite continuity and straightness among them) to navigate difficult regions of neuropil. Similarly, algorithms that agglomerate super-voxels make decisions on whether the resulting shape is more or less plausible on a medium length-scale. The required shape priors can either be designed using explicit knowledge about neurite shapes [22] or trained using the shapes of actual neurites [19,23]. Rather than considering one decision after another, one can consider the combined effect of multiple merge decisions to select a globally optimal set of mergers [9]. Now, back to single-voxel classification.

Flood-filling networks (FFNs), which are currently leading in segmentation performance [3[•],24], use an iterative voxel-classification process: first, using only the image intensities, an initial estimate for each voxel's probability of being part of the current neurite is generated. A feedback path makes the previous iteration's 'in'-probability part of the classifier input, automatically incorporating implicit shape priors into the primary voxel classification process.

Progress in VEM acquisition methods

Before we can start analyzing data we have to generate them. High-throughput VEM remains the state-of-the-art for resolving nanometer-sized structures, the development of sub-diffraction (super-resolution) light microscopy [25,26] and of methods that expand the tissue before imaging [27] notwithstanding. During the last decade, four VEM techniques were used for most connectomic

data sets (reviewed in [28]). Two of those techniques are based on serial block-face electron microscopy (SBEM). SBEM using a diamond knife (DiK-SBEM) was originally introduced more than three decades ago [29], but became an effective tool about a decade and a half ago when it was shown that it can be used on nervous tissue [30]. Since then SBEM data have been used to reconstruct neural circuits on a large scale (Table 1). A variant of SBEM was introduced that employs a focused ion beam (FIB) for the periodic removal of material from the block face [31,32]. With FIB-SBEM the resolution is improved in all directions. Block-face increments as low as 2 nm have been demonstrated [33[•]] (for DiK-SBEM, the thinnest layer that can be reliably removed is about 20 nm under realistic imaging conditions [17[•]]). The usable lateral resolution is almost on par with what can be achieved with TEM [33[•]], because FIB-based material removal tolerates a much larger electron exposure than DiK-SBEM [30]. The one big drawback of FIB-SBEM is that the field-of-view (FOV) is limited to a few tens of microns along the axis of the ion beam [32].

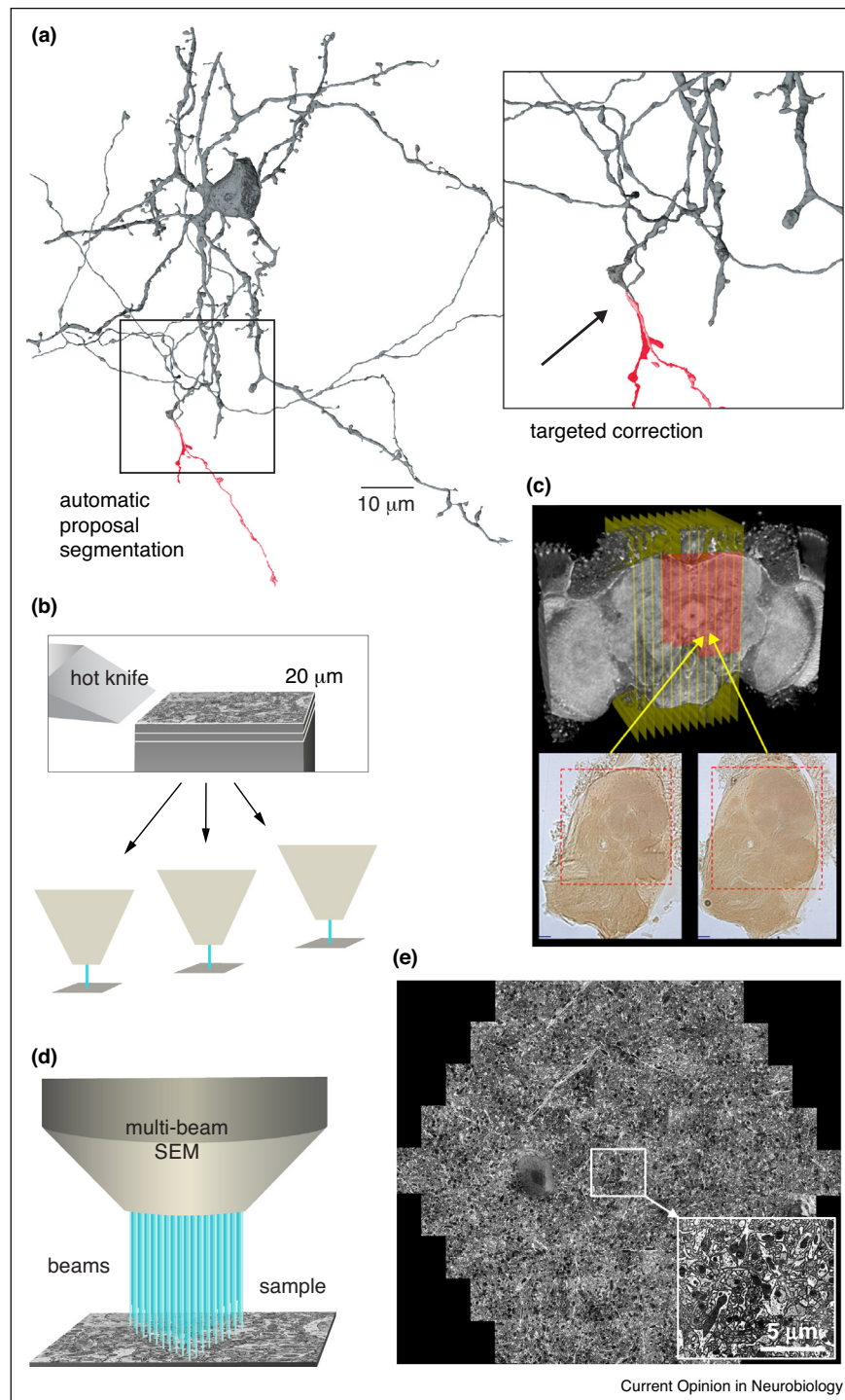
One of the most exciting recent advances in VEM was, therefore, the demonstration that epoxy-embedded heavy metal-stained brain-tissue samples can be cut — with only minimal loss of material at the interface — into slabs between 10 and 30 μm thick using a lubricated and heated diamond knife [34^{••}] (Figure 1b,c). By combining the hot-knife slab-cutting (HoKS?) technique with FIB-SBEM, a method (HoKS FIBSBEM?) is created that should have no limit on sample size (note that HoKS has not yet been demonstrated for mouse or bird whole-brain samples) and at the same time provides data that are of sufficient resolution and SNR to allow virtually error-free automatic neural circuit extraction [34^{••}].

It would take thousands of years to acquire FIB-SBEM data for a whole mouse (bird) brain with a single single-beam microscope, but if one takes advantage of the fact that the brain would be cut into hundreds or thousands of slabs, which can be imaged in parallel, the wall-clock time required can be reduced by simply using multiple machines, limited mainly by the available budget.

Setting budget issues aside for the moment, we could ask: Has any of the four approaches to VEM discussed by Briggman and Bock in their 2012 paper [28] emerged as the winner and is on the verge of making other approaches obsolete? Posing the question in a different way: if one were to embark on a large-scale effort to reconstruct one whole mouse (bird) brain now, is it time to commit to one of these approaches?

Based only on its track records, serial-section TEM (SSTEM) should be the method of choice (Table 1). SSTEM was used for all currently available whole-brain datasets: *C. elegans* with 302 neurons [18], the adult fruit

Figure 1



Progress in VEM analysis and data acquisition. **(a)** Surface rendering of an automatically generated neurite segmentation from the j0126 songbird data set (gray) and the missing part (red), reattached through targeted proofreading. **(b)** Hot-knife sample partitioning: Principle, **(c)** X-ray of *D. melanogaster* brain with superimposed hot-knife slice locations, adapted from [33*] (CC BY 4.0 license), and the multi-beam SEM: **(d)** schematic, **(e)** secondary electron image of a mouse brain section, adapted from [44**] (CC BY 4.0 license).

Table 1

Recent publications from connectomic VEM data sets

Discovery	Species	Brain area	VEM technique	Resolution [nm]	Data set size [TB]	Reconstruction method	Reference
Direction-specific wiring	Mouse	Retina	DiK-SBEM	17 × 17 × 23 and 12 × 12 × 25	1 and 0.13	Skeletonization	[21]
Random interneuron input	Mouse	V1 cortex	SSTEM	4 × 4 × 45	10	Skeletonization	[39]
Synaptic input competition at the Calyx of Held	Mouse	Medial nucleus of the trapezoid body	DiK-SBEM	6 × 6 × 60, 12 × 12 × 60, 10 × 10 × 60, 5 × 5 × 60, 5 × 5 × 40	0.9, 0.05, 0.06, 0.35, 1.05	Manual segmentation	[48]
Feeding network comparison	<i>P. pacificus</i> and <i>C. elegans</i>	Whole brain	SSTEM	50 and 70 thickness for <i>P. pacificus</i> and [18]		Skeletonization	[49]
Optic medulla connectome	Drosophila	Visual system	SSTEM	5000× magn., 40 nm sections	2	Segmentation + proofreading	[15]
New bipolar cell type	Mouse	Retina	DiK-SBEM	17 × 17 × 25 and [21]	0.19 and [21]	Segmentation + skeletonization	[10]
Amacrine cell network	Rabbit	Retina	SSTEM	2 × 2 × (70–90)	16.5	Skeletonization	[50]
Space-time wiring	Mouse	Retina	DiK-SBEM	[21]		Segmentation + proofreading	[51]
Cortical myelination profiles	Mouse	S1 and V1	ATUM	30 × 30 × 240 and [39]	0.14 and [39]	Manual segmentation	[52]
7-column medulla connectome	Drosophila	Visual system	FIB-SBEM	10 × 10 × 10	0.13	Segmentation + proofreading	[14]
Action selection for escape locomotion	Drosophila larva	a2/a3 and whole nervous system	SSTEM	4 × 4 × 45 and 4 × 4 × 50	0.2 and 2.4	Skeletonization	[36**]
Peter's rule violation	Mouse	Cortex	ATUM	3 × 3 × 29	0.3	Manual segmentation	[40]
Experience-based connectivity	Mouse	Visual thalamus	ATUM	4 × 4 × 30	100	Manual segmentation	[53]
Topological organization	Zebra fish larva	Olfactory bulb	DiK-SBEM	9 × 9 × 25	2.4	Skeletonization	[54]
Redundant synaptic connectivity across 'twigs'	Drosophila adult and larva	Visual and sensorimotor areas	SSTEM	[36**] and [15]		Skeletonization	[55]
Excitatory subnetworks	Mouse	V1	SSTEM	4 × 4 × 40	100	Skeletonization	[56]
Antennal lobe connectome	Drosophila larva	Whole nervous system	SSTEM	[36**]		Skeletonization	[57]
Hugin-neuron connectome	Drosophila larva	Whole nervous system	SSTEM	[36**]		Skeletonization	[58]
Role of competitive disinhibition in behavior regulation	Drosophila larva	Whole nervous system	SSTEM	[36**]		Skeletonization	[59]
Muscle activation wave circuitry	Drosophila larva	Whole nervous system	SSTEM	[36**]		Skeletonization	[60]
Recruitment of motor pools	Drosophila larva	Whole nervous system	SSTEM	[36**]		Skeletonization	[61]
Circuits conserved over development	Drosophila larva	Sensory areas L1v and L3v	SSTEM	2 × 2 × 50 and [36**]	5 and [36**]	Skeletonization	[62]
Mushroom body connectome	Drosophila	Mushroom body	FIB-SBEM	8 × 8 × 8	3.8	Segmentation + proofreading	[63]
Axonal synapse sorting	Zebra finch	HVC	DiK-SBEM	11 × 11 × 29	0.6	Skeletonization	[64]
Whole brain data set	Drosophila	Whole brain	SSTEM	4 × 4 × (35–40)	106		[35**]
Axonal synapse sorting	Rat	ME cortex	DiK-SBEM	11 × 11 × (30–50) and 11 × 11 × 30	12.6 and 1.1	Skeletonization	[65]
Mushroom body connectome	Drosophila larva	Mushroom body	SSTEM	[36**]		Skeletonization	[66]
Bilateral symmetry of myelinated axons	Zebrafish larva	Whole brain	ATUM	20 × 20 × 60	4.4	Skeletonization	[67*]
ORN to PN connectivity variations	Drosophila	Olfactory system	SSTEM	4 × 4 × 50	50	Skeletonization	[68]
ON motion detection T4 connectivity	Drosophila	Visual system	FIB-SBEM	[14]		Segmentation + Proofreading	[38]
Excitatory synapse clusters	Mouse	Hippocampus	SSTEM	4 × 4 × 50	1.5	Manual segmentation	[69]

Data set sizes were estimated, wherever necessary and possible, using provided volume dimensions and resolutions, or the number and size of image tiles, assuming 8-bit voxels.

fly (*D. melanogaster*) with approximately 250 000 neurons [35^{••}], and the larval fly nervous system with about 10 000 neurons [36^{••}].¹ SSTEM data are, however, more difficult to analyze automatically [33[•],38], likely due to the highly anisotropic resolution and to slice-to-slice jitter. Compare for example, reconstructions of the fly visual system based on SSTEM and FIB-SBEM data, respectively [14,15,38].

The FOV for TEM imaging needs to be contained within a single grid opening, across which the section has to be stably suspended and which cannot exceed the standard TEM grid's 3 mm outer diameter. This is too small for slices across a whole bird brain, which can be as large as 13 mm × 10 mm. But, as it did for FIB-SBEM [34^{••}], the hot knife may come to the rescue.

One reason for the continued popularity of TEM is that wide-field imaging is inherently parallel (scanning microscopes acquire data serially, one pixel at a time) allowing net imaging rates of about 50 MHz using a TEM that is read out with a camera array (TEMCA) [35^{••},39].

Does the automatic collection of ultrathin sections on tape (ATUM) [40,41], currently increasing in use (Table 1), have a future in connectomics? The resolution along the *z*-direction (somewhat lower than DiK-SBEM but way behind FIB-SBEM) could be improved by the acquisition of multiple images at different tilt angles or different landing energies. The missing information along the *z*-axis would then be recovered by tomographic reconstruction [42] or, multi-energy deconvolution [43], respectively. The ATUM's imaging speed depends on the scan rate of the SEM that is used, which for a single-beam instrument, is much behind that of TEMCA [35^{••}].

However, preparing the incoming electron beam in a way that results in a hexagonal array of high resolution foci (all scanned in synchrony) allows the acquisition from all these foci in parallel, as long as each focus is far enough from its closest neighbor to ensure separate secondary-electron detection. Such a multi-beam scanning electron microscope (MSEM) with up to 91 beams has been designed and is being sold by Carl Zeiss Microscopy (Figure 1d,e) [44^{••}]. So far, the MSEM has been used successfully on sections collected on a solid substrate (Kapton tape) using ATUM [45]. An attempt by one of us (WD) to combine MSEM and DiK-SBEM has run into unexpected difficulties (W Denk, unpublished observations). While a plausible idea for combining MSEM and FIB milling while maintaining a high overall image-

acquisition throughput has not appeared (at least not in our FOV), known difficulties being the slow speed of material removal and the need of the MSEM for a planar sample surface well beyond the border of the imaged area. The emergence of a mode of knife-less material removal that has a large FOV and leaves a smooth sample surface, gas cluster ion beam milling (K Hayworth *et al.*, accepted abstract, Microscopy and Microanalysis, Baltimore, August 2018), may be a way out.

Conclusion

We have taken the value of reconstructing circuit diagrams as being self-evident, needing neither introduction nor proof. After more than a decade of neo-connectomics (ignoring a century of neuroanatomy, including classical connectomics [18] and paleo-connectomics [46]), are we still mostly building (and refining and scaling up) the tools that will ultimately get us the all-powerful whole-brain data set(s)? Or are there already key insights of fundamental importance that one could not have been gained without the use of connectomics? We think that while there are some notable biological results (Table 1) we still need to remind ourselves of Amara's law [47], which tells us that the impact of novel technologies is almost always overestimated in the short term but underestimated in the long term. We are still confident that eventually the reading of memories and the discovery of new algorithmic principles will become the daily routine of connectomics.

Conflict of interest statement

None declared.

Acknowledgements

This research was supported by the Max Planck Society. We would like to thank Julia Kuhl for help with figure creation and Ken Hayworth for comments on the manuscript.

References and recommended reading

Papers of particular interest, published within the period of review, have been highlighted as:

- of special interest
- of outstanding interest

1. Dickmanns ED, Zapp A: **Autonomous high speed road vehicle guidance by computer vision**. *IFAC Proc Vol* 1987, **20**:221-226.
2. Seung HS: **Reading the book of memory: sparse sampling versus dense mapping of connectomes**. *Neuron* 2009, **62**:17-29.
3. Januszewski M, Kornfeld J, Li PH, Pope A, Blakely T, Lindsey L, •• Maitin-Shepard JB, Tyka M, Denk W, Jain V: **High-precision automated reconstruction of neurons with flood-filling networks**. *bioRxiv* 2017:200675.
4. Helmstaedter M, Briggman KL, Denk W: **High-accuracy neurite reconstruction for high-throughput neuroanatomy**. *Nat Neurosci* 2011, **14**:1081-1088.
5. Krasowski NE, Beier T, Knott GW, Kothe U, Hamprecht FA, Kreshuk A: **Neuron segmentation with high-level biological priors**. *IEEE Trans Med Imaging* 2018, **37**:829-839.

This paper shows that flood-filling neural networks (FFNs) can be successfully used to segment large volume EM data sets at high precision, implying greatly reduced proofreading effort. FFNs combine boundary detection and segmentation into a single neural network.

¹ Mostly for our own amusement, we took the numbers for *C. elegans* (~500) and the adult fruit fly (~250 000) to estimate the doubling time for the number of imaged neurons arriving at a value of 3.6 years (compared to about two years in the early decades of Moore's law [37]) which 'predicts' such data sets for mouse (bird) and human for the years 2049 and 2084, respectively, which may be too pessimistic.

6. Zador AM, Dubnau J, Oyibo HK, Zhan H, Cao G, Peikon ID: **Sequencing the connectome**. *PLoS Biol* 2012, **10**:e1001411.
 7. Yoon YG, Dai PL, Wohlwend J, Chang JB, Marblestone AH, Boyden ES: **Feasibility of 3D reconstruction of neural morphology using expansion microscopy and barcode-guided agglomeration**. *Front Comput Neurosci* 2017, **11**.
 8. Hagmann P, Kuntz M, Gigandet X, Thiran P, Wedeen VJ, Meuli R, Thiran JP: **Mapping human whole-brain structural networks with diffusion MRI**. *PLoS ONE* 2007, **2**:e597.
 9. Beier T, Pape C, Rahaman N, Prange T, Berg S, Bock DD, Cardona A, Knott GW, Plaza SM, Scheffer LK, Koethe U, Kreshuk A, Hamprecht FA: **Multicut brings automated neurite segmentation closer to human performance**. *Nat Methods* 2017, **14**:101-102.
 10. Helmstaedter M, Briggman KL, Turaga SC, Jain V, Seung HS, Denk W: **Connectomic reconstruction of the inner plexiform layer in the mouse retina**. *Nature* 2013, **500**:168-174.
 11. Turaga SC, Murray JF, Jain V, Roth F, Helmstaedter M, Briggman K, Denk W, Seung HS: **Convolutional networks can learn to generate affinity graphs for image segmentation**. *Neural Comput* 2010, **22**:511-538.
 12. Berning M, Boergens KM, Helmstaedter M: **SegEM: efficient image analysis for high-resolution connectomics**. *Neuron* 2015, **87**:1193-1206.
 13. Plaza SM: **Focused proofreading to reconstruct neural connectomes from EM images at scale**. *Lecture Notes in Computer Science (LNCS)* . 2016:249-258.
 14. Takemura SY, Xu CS, Lu Z, Rivlin PK, Parag T, Olbris DJ, Plaza S, Zhao T, Katz WT, Umayam L, Weaver C, Hess HF, Horne JA, Nunez-Iglesias J, Aniceto R, Chang LA, Lauchie S, Nasca A, Ogundeyi O, Sigmund C, Takemura S, Tran J, Langille C, Le Lacheur K, McLin S, Shinomiya A, Chklovskii DB, Meinertzhagen IA, Scheffer LK: **Synaptic circuits and their variations within different columns in the visual system of *Drosophila***. *Proc Natl Acad Sci U S A* 2015, **112**:13711-13716.
 15. Takemura SY, Bharioke A, Lu Z, Nern A, Vitaladevuni S, Rivlin PK, Katz WT, Olbris DJ, Plaza SM, Winston P, Zhao T, Horne JA, Fetter RD, Takemura S, Blazek K, Chang LA, Ogundeyi O, Saunders MA, Shapiro V, Sigmund C, Rubin GM, Scheffer LK, Meinertzhagen IA, Chklovskii DB: **A visual motion detection circuit suggested by *Drosophila* connectomics**. *Nature* 2013, **500**:175-181.
 16. Boergens KM, Berning M, Bocklisch T, Bräunlein D, Drawitsch F, Frohnhofer J, Herold T, Otto P, Rzepka N, Werkmeister T, Werner D, Wiese G, Wissler H, Helmstaedter M: **webKnossos: efficient online 3D data annotation for connectomics**. *Nat Methods* 2017, **14**:691-694.
 17. Dorkenwald S, Schubert PJ, Killinger MF, Urban G, Mikula S, Svava F, Kornfeld J: **Automated synaptic connectivity inference for volume electron microscopy**. *Nat Methods* 2017, **14**:435-442.
- This paper describes a computational pipeline that allows the automatic identification of synapses and generates an annotated connectivity matrix.
18. White JG, Southgate E, Thomson JN, Brenner S: **The structure of the nervous system of the nematode *Caenorhabditis elegans***. *Philos Trans R Soc Lond B Biol Sci* 1986, **314**:1-340.
 19. Rolnick D, Meirovitch Y, Parag T, Pfister H, Jain V, Lichtman JW, Boyden ES, Shavit N: **Morphological Error Detection in 3D Segmentations**. 2017 . arXiv preprint [arXiv:1705.10882](https://arxiv.org/abs/1705.10882).
 20. Zung J, Tartavull I, Seung HS: **An Error Detection and Correction Framework for Connectomics**. 2017 . arXiv preprint [arXiv:1708.02599](https://arxiv.org/abs/1708.02599).
 21. Briggman KL, Helmstaedter M, Denk W: **Wiring specificity in the direction-selectivity circuit of the retina**. *Nature* 2011, **471**:183-188.
 22. Nunez-Iglesias J, Kennedy R, Plaza SM, Chakraborty A, Katz WT: **Graph-based active learning of agglomeration (GALA): a Python library to segment 2D and 3D neuroimages**. *Front Neuroinf* 2014, **8**:34.
 23. Maitin-Shepard JB, Jain V, Januszewski M, Li P, Abbeel P: **Combinatorial Energy Learning for Image Segmentation**. 2016 . arXiv preprint [arXiv:1506.04304](https://arxiv.org/abs/1506.04304).
 24. Januszewski M, Maitin-Shepard J, Li P, Kornfeld J, Denk W, Jain V: **Flood-Filling Networks**. 2016 . arXiv preprint [arXiv:1611.00421](https://arxiv.org/abs/1611.00421).
 25. Klar TA, Jakobs S, Dyba M, Egner A, Hell SW: **Fluorescence microscopy with diffraction resolution barrier broken by stimulated emission**. *Proc Natl Acad Sci U S A* 2000, **97**:8206-8210.
 26. Betzig E, Patterson GH, Sougrat R, Lindwasser OW, Olenych S, Bonifacino JS, Davidson MW, Lippincott-Schwartz J, Hess HF: **Imaging intracellular fluorescent proteins at nanometer resolution**. *Science* 2006, **313**:1642-1645.
 27. Chen F, Tillberg PW, Boyden ES: **Optical imaging. Expansion microscopy**. *Science* 2015, **347**:543-548.
 28. Briggman KL, Bock DD: **Volume electron microscopy for neuronal circuit reconstruction**. *Curr Opin Neurobiol* 2012, **22**:154-161.
 29. Leighton SB: **SEM images of block faces, cut by a miniature microtome within the SEM – a technical note**. *Scan Electr Microsc* 1981:73-76.
 30. Denk W, Horstmann H: **Serial block-face scanning electron microscopy to reconstruct three-dimensional tissue nanostructure**. *PLoS Biol* 2004, **2**:e329.
 31. Heymann JA, Hayles M, Gestmann I, Giannuzzi LA, Lich B, Subramaniam S: **Site-specific 3D imaging of cells and tissues with a dual beam microscope**. *J Struct Biol* 2006, **155**:63-73.
 32. Knott G, Marchman H, Wall D, Lich B: **Serial section scanning electron microscopy of adult brain tissue using focused ion beam milling**. *J Neurosci* 2008, **28**:2959-2964.
 33. Xu CS, Hayworth KJ, Lu Z, Grob P, Hassan AM, Garcia-Cerdan JG, Niyogi KK, Nogales E, Weinberg RJ, Hess HF: **Enhanced FIB-SEM systems for large-volume 3D imaging**. *Elife* 2017, **6**.
- This paper shows that to acquire volume electron microscopy data of a large tissue piece by pairing it with the hot-knife technique and increasing the stability and reliability of the image acquisition pipeline. FIB-SEM was limited by slow imaging speeds and a lack of long-term stability. The authors present several solutions to overcome these difficulties and demonstrate that data sets of up to at least $10^6 \mu\text{m}^3$ can be acquired at 8 nm isotropic resolution.
34. Hayworth KJ, Xu CS, Lu Z, Knott GW, Fetter RD, Tapia JC, Lichtman JW, Hess HF: **Ultrastructurally smooth thick partitioning and volume stitching for large-scale connectomics**. *Nat Methods* 2015, **12**:319-322.
- This paper introduces a method that uses a heated diamond knife to partition large tissue samples into pieces, with only minor data loss at the interfaces. Each piece can be imaged by FIB-SEM at high-resolution. This allows parallelization of FIB-SEM and scaling up to large volumes.
35. Zheng Z, Lauritzen JS, Perlman E, Robinson CG, Nichols M, Milkie D, Torrens O, Price J, Fisher CB, Sharifi N, Calle-Schuler SA, Kmecova L, Ali IJ, Karsh B, Trautman ET, Bogovic J, Hanslovsky P, Jefferis GSXE, Kazhdan M, Khairy K, Saalfeld S, Fetter RD, Bock DD: **A complete electron microscopy volume of the brain of adult *Drosophila melanogaster***. *bioRxiv* 2017:140905.
- This paper describes a SSTEM data set of a complete *D. melanogaster* brain, using a second-generation camera array (TEMCA).
36. Ohyama T, Schneider-Mizell CM, Fetter RD, Aleman JV, Franconville R, Rivera-Alba M, Mensh BD, Branson KM, Simpson JH, Truman JW, Cardona A, Zlatić M: **A multilevel multimodal circuit enhances action selection in *Drosophila***. *Nature* 2015, **520**:633-639.
- A whole *D. melanogaster* larval nervous system SSTEM data set was acquired, enabling the identification of multilevel multimodal circuits for action selection in escape responses.
37. Schaller RR: **Moore's law: past, present, and future**. *IEEE Spectr* 1997, **34**:52-59.
 38. Takemura SY, Nern A, Chklovskii DB, Scheffer LK, Rubin GM, Meinertzhagen IA: **The comprehensive connectome of a neural substrate for 'ON' motion detection in *Drosophila***. *Elife* 2017, **6**.

39. Bock DD, Lee WC, Kerlin AM, Andermann ML, Hood G, Wetzel AW, Yurgenson S, Soucy ER, Kim HS, Reid RC: **Network anatomy and in vivo physiology of visual cortical neurons.** *Nature* 2011, **471**:177-182.
 40. Kasthuri N, Hayworth KJ, Berger DR, Schalek RL, Conchello JA, Knowles-Barley S, Lee D, Vazquez-Reina A, Kaynig V, Jones TR, Roberts M, Morgan JL, Tapia JC, Seung HS, Roncal WG, Vogelstein JT, Burns R, Sussman DL, Priebe CE, Pfister H, Lichtman JW: **Saturated reconstruction of a volume of neocortex.** *Cell* 2015, **162**:648-661.
 41. Hayworth KJ, Kasthuri N, Schalek R, Lichtman JW: **Automating the collection of ultrathin serial sections for large volume TEM reconstructions.** *Microsc Microanal* 2006, **12**:86-87.
 42. Gilbert PF: **The reconstruction of a three-dimensional structure from projections and its application to electron microscopy. II. Direct methods.** *Proc R Soc Lond B Biol Sci* 1972, **182**:89-102.
 43. Boughorbel F, Zhuge X, Potocek P, Lich B: **SEM 3D reconstruction of stained bulk bio samples using landing energy variation and deconvolution.** *Microsc Microanal* 2012, **18**:560-561.
 44. Eberle AL, Mikula S, Schalek R, Lichtman J, Knothe Tate ML, ●● Zeidler D: **High-resolution, high-throughput imaging with a multibeam scanning electron microscope.** *J Microsc* 2015, **259**:114-120.
- A novel multi-beam scanning electron microscope is introduced that scans the sample with multiple beams in parallel and thus increases the aggregate imaging throughput by 2 orders of magnitude compared to a single beam. High quality imaging of brain samples is demonstrated.
45. Schalek R, Lee D, Kasthuri N, Peleg A, Jones T, Kaynig V, Haehn D, Pfister H, Cox D, Lichtman J: **Imaging a 1 mm³ volume of rat cortex using a multi beam SEM.** *Microsc Microanal* 2016, **22**:582-583.
 46. Cajal RS: **Estructura de los centros nerviosos de las aves.** *RevTrimest Histol Norm Patol* 1888, **1**.
 47. Ratcliffe S: *Oxford Essential Quotations*. edn 5. Oxford University Press; 2016.
 48. Holcomb PS, Hoffpauir BK, Hoyson MC, Jackson DR, Deerinck TJ, Marrs GS, Dehoff M, Wu J, Ellisman MH, Spirou GA: **Synaptic inputs compete during rapid formation of the calyx of Held: a new model system for neural development.** *J Neurosci* 2013, **33**:12954-12969.
 49. Bumbarger DJ, Riebesell M, Rodelsperger C, Sommer RJ: **System-wide rewiring underlies behavioral differences in predatory and bacterial-feeding nematodes.** *Cell* 2013, **152**:109-119.
 50. Marc RE, Anderson JR, Jones BW, Sigulinsky CL, Lauritzen JS: **The All amacrine cell connectome: a dense network hub.** *Front Neural Circ* 2014, **8**:104.
 51. Kim JS, Greene MJ, Zlateski A, Lee K, Richardson M, Turaga SC, Purcaro M, Balkam M, Robinson A, Behabadi BF, Campos M, Denk W, Seung HS, Lichtman JW, Arlotta P: **Distinct profiles of myelin distribution along single axons of pyramidal neurons in the neocortex.** *Science* 2014, **344**:319-324.
 52. Tomassy GS, Berger DR, Chen HH, Kasthuri N, Hayworth KJ, Vercelli A, Seung HS, Lichtman JW, Arlotta P: **Distinct profiles of myelin distribution along single axons of pyramidal neurons in the neocortex.** *Science* 2014, **344**:319-324.
 53. Morgan JL, Berger DR, Wetzel AW, Lichtman JW: **The fuzzy logic of network connectivity in mouse visual thalamus.** *Cell* 2016, **165**:192-206.
 54. Wanner AA, Genoud C, Masudi T, Siksou L, Friedrich RW: **Dense EM-based reconstruction of the interglomerular projectome in the zebrafish olfactory bulb.** *Nat Neurosci* 2016, **19**:816-825.
 55. Schneider-Mizell CM, Gerhard S, Longair M, Kazimiers T, Li F, Zwart MF, Champion A, Midgley FM, Fetter RD, Saalfeld S, Cardona A: **Quantitative neuroanatomy for connectomics in Drosophila.** *Elife* 2016, **5**.
 56. Lee WC, Bonin V, Reed M, Graham BJ, Hood G, Glattfelder K, Reid RC: **Anatomy and function of an excitatory network in the visual cortex.** *Nature* 2016, **532**:370-374.
 57. Berck ME, Khandelwal A, Claus L, Hernandez-Nunez L, Si G, Tabone CJ, Li F, Truman JW, Fetter RD, Louis M, Samuel AD, Cardona A: **The wiring diagram of a glomerular olfactory system.** *Elife* 2016, **5**.
 58. Schlegel P, Texada MJ, Miroshchnikov A, Schoofs A, Hucksfeld S, Peters M, Schneider-Mizell CM, Lacin H, Li F, Fetter RD, Truman JW, Cardona A, Pankratz MJ: **Synaptic transmission parallels neuromodulation in a central food-intake circuit.** *Elife* 2016, **5**.
 59. Jovanic T, Schneider-Mizell CM, Shao M, Masson JB, Denisov G, Fetter RD, Mensh BD, Truman JW, Cardona A, Zlatić M: **Competitive disinhibition mediates behavioral choice and sequences in Drosophila.** *Cell* 2016, **167**:858-870.e819.
 60. Fushiki A, Zwart MF, Kohsaka H, Fetter RD, Cardona A, Nose A: **A circuit mechanism for the propagation of waves of muscle contraction in Drosophila.** *Elife* 2016, **5**.
 61. Zwart MF, Pulver SR, Truman JW, Fushiki A, Fetter RD, Cardona A, Landgraf M: **Selective inhibition mediates the sequential recruitment of motor pools.** *Neuron* 2016, **91**:944.
 62. Gerhard S, Andrade I, Fetter RD, Cardona A, Schneider-Mizell CM: **Conserved neural circuit structure across Drosophila larva development revealed by comparative connectomics.** *Elife* 2017, **6**.
 63. Takemura SY, Aso Y, Hige T, Wong A, Lu Z, Xu CS, Rivlin PK, Hess H, Zhao T, Parag T, Berg S, Huang G, Katz W, Olbris DJ, Plaza S, Umayam L, Aniceto R, Chang LA, Lauchie S, Ogundeyi O, Ordish C, Shinomiya A, Sigmund C, Takemura S, Tran J, Turner GC, Rubin GM, Scheffer LK: **A connectome of a learning and memory center in the adult Drosophila brain.** *Elife* 2017, **6**.
 64. Kornfeld J, Benezra SE, Narayanan RT, Svava F, Egger R, Oberlaender M, Denk W, Long MA: **EM connectomics reveals axonal target variation in a sequence-generating network.** *Elife* 2017, **6**.
 65. Schmidt H, Gour A, Straehle J, Boergens KM, Brecht M, Helmstaedter M: **Axonal synapse sorting in medial entorhinal cortex.** *Nature* 2017, **549**:469-475.
 66. Eichler K, Li F, Litwin-Kumar A, Park Y, Andrade I, Schneider-Mizell CM, Saumweber T, Huser A, Eschbach C, Gerber B, Fetter RD, Truman JW, Priebe CE, Abbott LF, Thum AS, Zlatić M, Cardona A: **The complete connectome of a learning and memory centre in an insect brain.** *Nature* 2017, **548**:175-182.
 67. Hildebrand DGC, Cicconet M, Torres RM, Choi W, Quan TM, ● Moon J, Wetzel AW, Scott Champion A, Graham BJ, Randlett O, Plummer GS, Portugues R, Bianco IH, Saalfeld S, Baden AD, Lillaney K, Burns R, Vogelstein JT, Schier AF, Lee WA, Jeong WK, Lichtman JW, Engert F: **Whole-brain serial-section electron microscopy in larval zebrafish.** *Nature* 2017, **545**:345-349.
- This paper describes a larval zebra fish whole brain data set that was acquired using ATUM. It also describes targeted, high-resolution reimagining of a set of sections after a complete lower resolution imaging pass.
68. Tobin WF, Wilson RI, Lee W-CA: **Wiring variations that enable and constrain neural computation in a sensory microcircuit.** *Elife* 2017, **6**.
 69. Bloss EB, Cembrowski MS, Karsh B, Colonell J, Fetter RD, Spruston N: **Single excitatory axons form clustered synapses onto CA1 pyramidal cell dendrites.** *Nat Neurosci* 2018, **21**:353-363.